Revealing Hofstadter spectrum for graphene in a periodic potential

Godfrey Gumbs,[1,2] Andrii Iurov,[1,*] Danhong Huang,[3] and Liubov Zhemchuzhna[4]

[1]*Department of Physics and Astronomy, Hunter College of the City University of New York, 695 Park Avenue, New York, New York 10065, USA*
[2]*Donostia International Physics Center (DIPC), Paseo Manuel de Lardizabal 4, 20018 San Sebastian, Basque Country, Spain*
[3]*Air Force Research Laboratory, Space Vehicles Directorate, Kirtland Air Force Base, New Mexico 87117, USA*
[4]*Department of Math & Physics, North Carolina Central University, Durham, North Carolina 27707, USA*

We calculate the energy bands for graphene monolayers when electrons move through a periodic electrostatic potential in the presence of a uniform perpendicular magnetic field. We clearly demonstrate the quantum fractal nature of the energy bands at reasonably low magnetic fields. We present results for the energy bands as functions of both wave number and magnetic flux through the unit cells of the resulting moiré superlattice. The effects due to pseudospin coupling and Landau orbit mixing by a strong scattering potential have been exhibited. At low magnetic fields when the Landau orbits are much larger than the period of the modulation, the Landau levels are only slightly broadened. This feature is also observed at extremely high magnetic fields. The density of states has been calculated and shows a remarkable self-similarity like the energy bands. We estimate that for modulation period of 10 nm the region where the Hofstadter butterfly is revealed is $B \leqslant 2$ T.

I. INTRODUCTION

In recent experiments [1–3], graphene flake and bilayer graphene were coupled to a rotationally aligned hexagonal boron nitride substrate. The spatially varying interlayer electrostatic potential gives rise to local symmetry breaking of the carbon sublattice as well as a long-range moiré superlattice potential in the graphene layer. At high magnetic fields, integer conductance plateaus which were obtained at noninteger filling factors were believed to be due to the formation of the Hofstadter butterfly in a symmetry-broken Landau level. These experiments were partially motivated by the pioneering theoretical work of Azbel [4] and Hofstadter [5] on the single-particle spectrum of a two-dimensional structure in the presence of both a periodic potential and a uniform ambient perpendicular magnetic field. In this case, the energies exhibit a self-similar recursive energy spectrum. There are several other effects due to the presence of boron nitride substrate. The band gaps, which appear in graphene due to the substrate, were theoretically modeled in [6]. The existence of a commensurate state, when the crystal is adjusted by the presence of the external periodic potential, has been investigated in [7]. Hofstadter fractal structures may also be realized in a variety of systems, such as Jaynes-Cummings-Hubbard lattices [8]. We should also mention a recent study of the energy spectrum of Schrödinger electrons, subjected to general periodic potential and magnetic field [9].

We note that the Hofstadter butterfly spectrum in moiré superlattices has been demonstrated to be a possibility for twisted bilayer graphene at achievable magnetic fields. The opportunity to observe the Hofstadter pattern at lower than previously predicted magnetic fields values provides experimentalists with an alternative structure to observe the Hofstadter butterfly. The band structure and the quantum Hall effect for twisted bilayer graphene having various rotation angles in the presence of magnetic field were investigated in

[10–12]. The low-energy band, quantized into Landau levels in accordance with the structure of the folded energy band, evolves into a Hofstadter spectrum as the magnetic field is increased. However, this effect which is also obtained in the presence of modulation applied to a flat graphene sample differs in a significant way from twisted bilayer graphene. The reason is that only the component of magnetic field perpendicular to the surface of twisted bilayer graphene has any effect on the electrons thereby making its presence felt nonuniformly unlike the case of modulated graphene. Landau quantization of the electronic spectrum for twisted graphene bilayers was also addressed in [13].

The fractal nature of the Hofstadter butterfly had captivated researchers for many years [14–30]. The paper by Hofstadter [5] was for the energy spectrum of a periodic square lattice in the tight-binding approximation and subject to a perpendicular magnetic field. Ever since that time, there have been complementary calculations for the hexagonal lattice [14], the two-dimensional electron gas (2DEG) with an electrostatic periodic modulation potential [21,22,30], and even bilayer graphene where different stacking of the two types of atoms forming the sublattices was considered [31]. It has been claimed that one may be able to observe evidence of the existence of Hofstadter's butterfly in such experimentally measured quantities as density of states and conductivity of the 2DEG [2,3,33].

The challenge facing experimentalists had been to carry out experiments on 2D structures at achievable magnetic fields where the Hofstadter butterfly spectrum is predicted. However, both monolayer and bilayer graphene coupled to hexagonal boron nitride provide a nearly ideal-sized periodic modulation, enabling unprecedented experimental access to the fractal spectrum [1–3].

In formulating a theoretical framework for the energy band structure for a periodically modulated energy band structure in a uniform magnetic field, one may adopt the procedure of Hofstadter by using Harper's equation which may be viewed as a tight-binding approximation of the Schrödinger equation. Additionally, assuming that the magnetic flux through the unit

---

*theorist.physics@gmail.com

cell of the periodic lattice is a rational fraction p/q of the flux quantum in conjunction with the Bloch condition for the wave function, one obtains a $p \times p$ Hamiltonian matrix to determine the energy eigenvalues since one only needs to solve the problem in a unit cell. Hofstadter himself was concerned about ever reaching magnetic fields where the rich self-similar structure of the butterfly would be experimentally observed due to the estimated high fields required to achieve this.

In this Rapid Communication, we supplement the recent experimental work on graphene by first presenting a formalism for calculating the energy band structure when an electrostatic modulation potential is applied to a flat sheet in the presence of a reasonably low perpendicular magnetic field. These results are then employed in a calculation of the density of states (DoS). Our results may be verified experimentally since the DoS is directly proportional to the quantum capacitance [32]. The DoS may also be obtained from magnetic susceptibility measurements. For a review of related energy band structure studies, see [29]. We also compare our results with those for a modulated two-dimensional electron gas and discuss the difference. The papers by Hunt *et al.* [1], Dean *et al.* [2], and Ponomarenko *et al.* [3] provided some encouragement that the Hofstadter butterfly can be realized and a theoretical formalism for the energy band structure of graphitic materials should be welcome. Our method of calculations for the Hofstadter spectrum may be extended to explain the ballistic transport properties, presented in Refs. [1–3] to complement our results for DoS.

II. GENERAL FORMULATION OF THE PROBLEM

In the presence of a uniform perpendicular magnetic field B_0 and periodic two-dimensional electrostatic modulation potential defined by [30]

$$\mathbb{V}(x, y) = \mathbb{V}_0 \left[\cos\left(\frac{\pi x}{d_x}\right) \cos\left(\frac{\pi y}{d_y}\right) \right]^{2N}, \quad (1)$$

where $N = 1, 2, \ldots$ is an integer determining the size of the scatterers, the parameter $\mathbb{V}_0$ is the modulation amplitude, and d_x, d_y are the modulation periods in the x and y directions, respectively, we rewrite the Hamiltonian operator as

$$\mathcal{H} = \begin{bmatrix} \mathbb{V}(x,y) & \hat{p}_x + eB_0 y \hat{x}_0 + \iota \hat{p}_y \\ \hat{p}_x + eB_0 y \hat{x}_0 - \iota \hat{p}_y & \mathbb{V}(x,y) \end{bmatrix}. \quad (2)$$

For this new system, the magnetic flux per unit cell is $\Phi = B_0(d_x d_y)$, which is assumed to be a rational fraction of the flux quantum $\Phi_0 = \hbar/e$; i.e., $\beta \equiv \Phi/\Phi_0 = p/q$, where p and q are prime integers. Furthermore, we choose the first Brillouin zone defined by $|k_x| \leqslant \pi/d_x$ and $|k_y| \leqslant \pi/(q d_y)$.

By using the Bloch-Peierls condition, the wave function of this system may be expanded as

$$\Phi_{\ell;n,\vec{k}_{\|}}^{\pm}(x, y) = \frac{1}{\sqrt{2\mathcal{N}_y}} \sum_{s=-\infty}^{\infty} e^{ik_y \ell_B^2 (sp+\ell)K_1} \Psi_{n,k_x-(sp+\ell)K_1}^{K,\pm}(x, y),$$

$$(3)$$

where $\vec{k}_{\|} = (k_x, k_y)$, $\mathcal{N}_y = L_y/(q d_y)$ is the number of unit cells, which are spanned by $b_1 = (d_x, 0)$ and $b_2 = (0, q d_y)$, in the y direction, $L_y (\to \infty)$ is the sample length in the y direction, $K_1 = 2\pi/d_x$ is the reciprocal lattice vector in the

x direction, and $\ell = 1, 2, \ldots, p$ is a new quantum number for labeling split p subbands from a k_x-degenerated Landau level in the absence of modulation. The above wave function satisfies the usual Bloch condition:

$$\Phi_{\ell;n,\vec{k}_{\|}}^{\pm}(x + d_x, y + q d_y) = e^{ik_x d_x} e^{ik_y q d_y} \Phi_{\ell;n,k_{\|}}^{\pm}(x, y). \quad (4)$$

Since the wave functions at K and K' points are decoupled from each other for monolayer graphene, which is different from bilayer graphene [34], we can write out explicitly the full expression for the wave function at these two points. A tedious but straightforward calculation yields the magnetic band structure for this modulated system as a solution of the eigenvector problem $\mathcal{M} \otimes \vec{\mathcal{A}}(\vec{k}_{\|}) = 0$ with the coefficient matrix $\overset{\leftrightarrow}{\mathcal{M}}$ given by

$$\{\mathcal{M}\}_{j, j'} = \left[E_n^\mu - \varepsilon(\vec{k}_{\|}) \right] \delta_{n,n'} \delta_{\ell,\ell'} \delta_{\mu,\mu'}^{(n)} + \mathbb{V}_{\ell,n,\mu}^{\ell',n',\mu'}(\vec{k}_{\|}), \quad (5)$$

where $\delta_{\mu,\mu'}^{(n)} = 1$ for $n = 0$ and $\delta_{\mu,\mu'}^{(n)} = \delta_{\mu,\mu'}$ for $n > 0$, $j = \{n, \ell, \mu\}$ is the composite index, and $\{\vec{\mathcal{A}}(\vec{k}_{\|})\}_j = \mathcal{A}_{n,\ell}^\mu(\vec{k}_{\|})$ is the eigenvector. The eigenvalue $\varepsilon_\nu(\vec{k}_{\|})$ of the system is determined by $\text{Det}\{\overset{\leftrightarrow}{\mathcal{M}}\} = 0$. Here we calculate $\mathbb{V}_{\ell,n,\mu}^{\ell',n',\mu'}(\vec{k}_{\|})$ as the Fourier transform. The detailed derivation of these matrix elements could be found in [35].

III. NUMERICAL RESULTS AND DISCUSSION

The Hofstadter spectrum evolves from degenerate Landau levels as the magnetic field is increased when applied to either modulated graphene or the 2DEG. This modification does not result in isomorphic graphs in the sense that one may be mapped onto the other with one-to-one correspondence. In particular, the highest energy levels expand at different rates for the two systems. Figure 1 shows that for a 2DEG, the lowest perturbed Landau subband which originates from the unperturbed $n = 0$ Landau level merges with the emerging
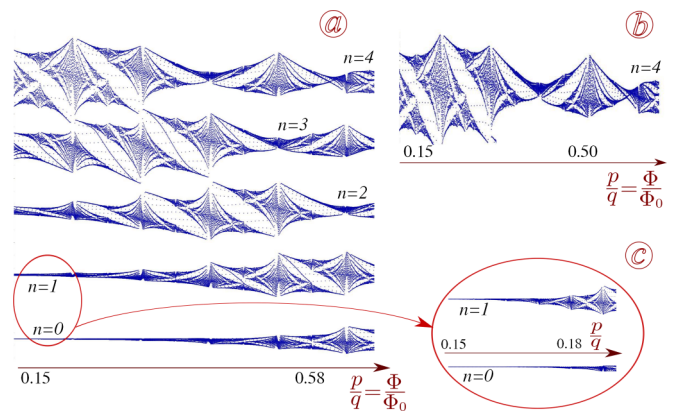

FIG. 1. (Color online) Energy band structure of a weakly modulated 2DEG as a function of magnetic flux ratio p/q. Panel (a) presents the four lowest Landau subbands for chosen modulation strength $\mathbb{V}_0 = 0.5 \hbar\omega_c$, $N = 10$, and $k_x = k_y = 0.3$ in units of $2\pi/d_x$. Panel (b) shows the detailed band structure of the $n = 4$ Landau level for a 2DEG. Panel (c) shows a zoom-in of the low-field portion of the two lowest levels for a 2DEG, demonstrating self-repeated structures for all levels and magnetic field.
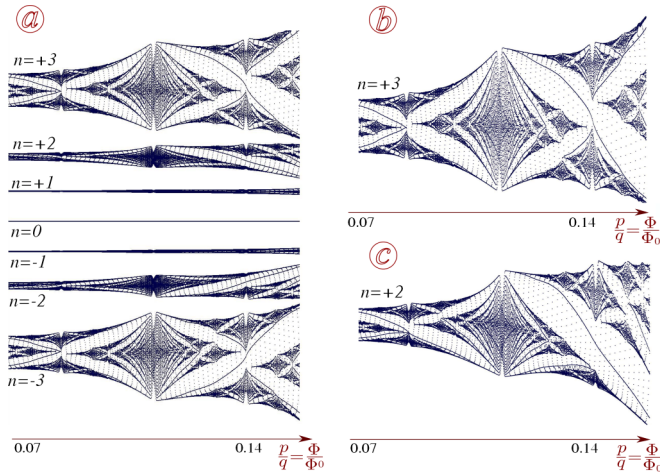
FIG. 2. (Color online) Band structure of strongly modulated graphene as a function of magnetic flux ratio p/q. Panel (a) gives the lowest few Landau subbands from both valence and conduction bands for a chosen modulation $\mathbb{V}_0 = 2.0\,\hbar\omega_c$ and $k_x = k_y = 0.3/d_x$. Panels (b) and (c) show details of the band structure of the $n = +2$ and $n = +3$ Landau levels. The levels are not mixed.

butterfly spectrum at the highest magnetic field compared to the $n = 1,2,3,4$ Landau levels in the conduction band. The onset of the butterfly takes place around $p/q = 1/5$ which would correspond to a magnetic field $B \approx 2$ T for $d_x = d_y = 10$ nm. Modulated 2DEG is special in the sense that for weak $\mathbb{V}_0$ the Landau subbands do not overlap, which is in contrast with graphene where the overlap always takes place, except for the few lowest subbands, which are shown in Fig. 2. Furthermore, our calculations have shown that for graphene the symmetry between the valence and conduction bands is destroyed by modulation. There is always mixing of the subbands regardless of the value for $\mathbb{V}_0$. The lowest subband is shifted upward like the other subbands but is not widened as much as the higher subbands. The feature of self-similarity is also apparent in the excited subbands at intermediate and high magnetic fields. There is only a shift and broadening of the subbands in the low and high magnetic field regimes for modulated 2DEG. We note that in order to obtain self-repeated fractal Hofstadter pattern, which obviously reveals a pattern of symmetry, we ought to plot the energy subbands using a scaling procedure outlined as follows: $\mathbb{E}_n = \{\epsilon_n - \mathbb{V}_0 \mathbb{C}_n^2(1 + \mathbb{A}_n)[(2N)!/(N!)^2]^2/4^2 N\}(\hbar\omega_c)^{-1}$, where $\mathbb{A}_n = (1 - \delta_{n,0})$ and $\mathbb{C}_n = \delta_{n,0} + (1 - \delta_{n,0})/\sqrt{2}$, where $2N$ is the power of the modulation potential function and $\mathbb{V}_0$ is the modulation amplitude. This scaling is appropriate for modulated electronic systems. A similar prescription for the 2DEG Hofstadter bands was used in [30], although the corresponding eigenvalue equation is different. This discussion is applicable for nonscaled subbands.

The results of our calculations for the energy eigenvalues of modulated graphene as a function of magnetic flux appear in Fig. 2. For weak magnetic fields, the Landau levels in both valence and conduction bands are slightly broadened into narrow subbands but shifted upward by the perturbing potential $\mathbb{V}_0$. Another effect due to modulation is to cause these unscaled Landau subbands to have negative slope at weak magnetic
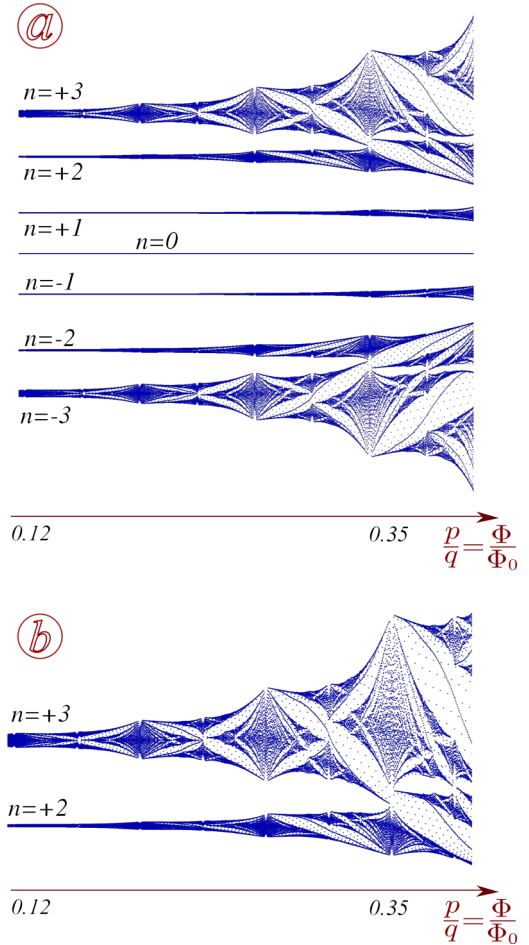

FIG. 3. (Color online) Band structure of a modulated graphene monolayer as a function of magnetic (flux ratio p/q). Panel (a) demonstrates the lowest few Landau subbands from both valence and conduction bands for a chosen modulation $\mathbb{V}_0 = 5.0\,\hbar\omega_c$ and $k_x = k_y = 0.3$. Panels (b) and (c) show the structure of ($n = +2$) and ($n = +3$) Landau levels. The levels are mixed.

fields which then broaden enough at higher magnetic fields to produce Landau orbit mixing, reflecting the commensurability effect for the magnetic and lattice Brillouin zones. In Fig. 3, we demonstrate a Hofstadter dispersion plot for the case when at least two Landau levels are mixed, featuring a larger fractal self-repeated structure, which incorporates more than one energy level.

In Fig. 4, we present the dispersion curves as a function of $k_x d_x$ for chosen value of $\mathbb{V}_0$ and two pairs of values of p and q corresponding to two different magnetic field strengths. In each case, there are p Landau subbands; q/p determines the number of oscillation periods in the first Brillouin zone for each of these subbands. Both the valence and conduction subbands are shifted upward but the conduction subbands are proportionally shifted more than the valence subbands for each corresponding Landau label for the unmodulated structure. This shift is increased when the modulation amplitude is increased. The original zero-energy Landau level is only slightly broadened and is the least affected by $\mathbb{V}_0$. If the sign of the modulation amplitude is reversed to correspond to an array of quantum dots, then the subbands are all shifted
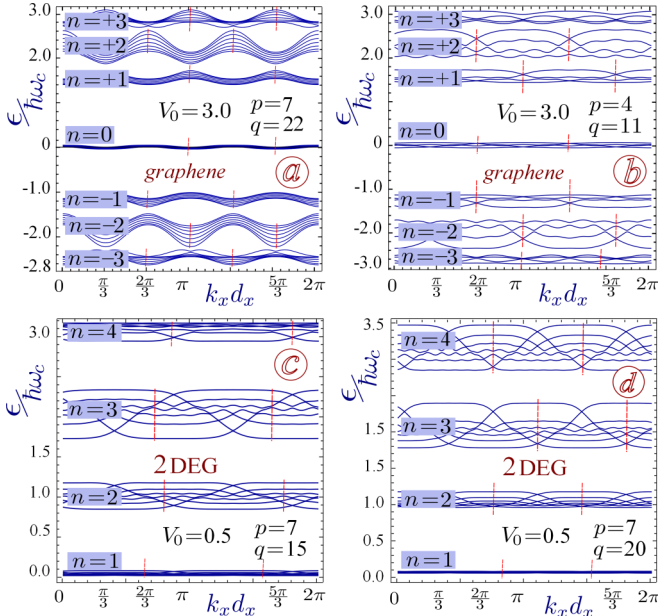
FIG. 4. (Color online) Energy dispersion as functions of $k_x d_x$ for graphene and 2DEG with chosen values of modulation potential $\mathbb{V}_0$ and magnetic flux p/q in units of the flux quantum. The energy is scaled in terms of $v_F \sqrt{Be\hbar}$.

downward from their positions for an unmodulated monolayer graphene.

We also calculate and display the density-of-states plots, which demonstrate the general magnetic field dependence of the Hofstadter spectrum, showing the general fractal structures independent of the specific values of the wave vector $\vec{k}_\parallel$. Based on the calculated eigenenergy $\varepsilon_\nu(\vec{k}_\parallel)$, we can further calculate the electron density of states in this system, given by

$$\rho(\varepsilon, B_0) = \frac{1}{2\pi^2 q d_x d_y} \sum_\nu \int_{-\pi/d_x}^{\pi/d_x} dk_x$$

$$\times \int_{-\pi/(q d_y)}^{\pi/(q d_y)} dk_y \frac{\Gamma/\pi}{[\varepsilon - \varepsilon_\nu(\vec{k}_\parallel)]^2 + \Gamma^2}, \quad (6)$$

where Γ represents the level broadening. Making use of our calculated energy eigenvalues $\epsilon_\nu(\vec{k})$, we further determine the electron density of states for monolayer graphene in the presence of a uniform perpendicular magnetic field.

A plot of the density of states as a function of magnetic field basically reproduces the Hofstadter self-repeating fractal structure, averaged over all allowed values of $\vec{k}$. In our calculations, the delta function is chosen as a Lorentzian. This leads to the finite width for the density of states for various values of energy ϵ. In this regard, one should look at Ref. [36], in which the density of states has been calculated for carbon nanotubes for the various cases of magnetic field strength and orientation.

Figure 5 shows $\rho(\epsilon, B) B$. We chose this specific set of results obtained for the density-of-states to demonstrate the effect due to the modulation in order to show how the Hofstadter structure may be suppressed by the strong δ-like peaks at low magnetic fields.
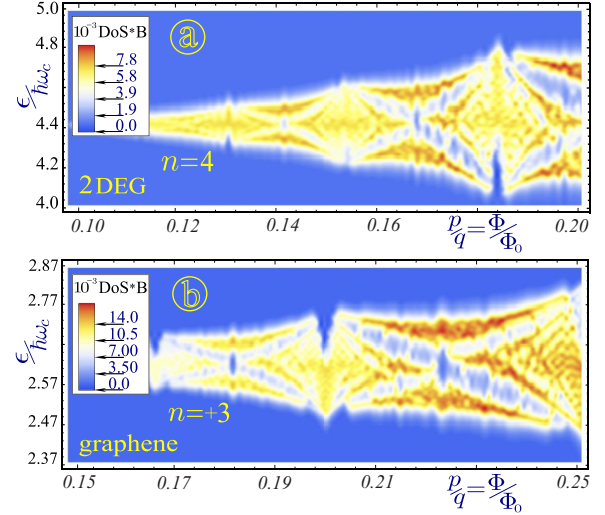

FIG. 5. (Color online) Density-of-states plots for modulated 2DEG and graphene. Panel (a) shows the density of states for a 2DEG with modulation $\mathbb{V}_0 = 0.5 \hbar\omega_c$ and modulation parameter $N = 5$. Panel (b) demonstrates the corresponding situation for graphene with $\mathbb{V}_0 = 1.5 \hbar\omega_c$ and $N = 3$. For both (a) and (b), the density-of-states amplitude is increased proportionally to the value of magnetic field in order to make the Hofstadter structure visible at large fields.

With regard to the effect of the electrostatic modulation on the Hofstadter spectrum, we would like to comment on how the standard Dirac cone type of energy dispersion would be modified in the presence of modulation only, without the magnetic field. This situation could be described by the following Hamiltonian: $\mathcal{H}_\mathbb{V} = \sigma \cdot \mathbf{p} + \mathbb{V}(x,y)\mathcal{I}$ with $\mathbb{V}(x,y)$ given in Eq. (1) and $\mathcal{I}$ is the unit matrix. Obviously, we are dealing with the continuous spectrum, accompanied generally by a strong anisotropic dependence on k_x and k_y wave numbers. The wave function, corresponding to such periodic potential also satisfied the Bloch condition (4). Such a Hamiltonian with a periodic potential in one dimension was considered in [37]. Their results show that new zero energy states emerge and the wave function corresponds to an overdamped particle in a periodic potential. These zero energy solutions in fact represent new Dirac points. The presence of the zero-averaged wave number gaps as well as extra Dirac points in the band structure for the graphene-based one-dimensional superlattices were also found in [38]. The effect of nonhomogeneous magnetic and electric fields was addressed in [39]. Consideration of one-dimensional modulation, as discussed in Ref. [40], could lead to novel energy dispersions.

IV. CONCLUSIONS

In summary, the well established Dirac fermion model is utilized to investigate the Landau level spectra of monolayer graphene in the presence of a periodic electrostatic potential. The intrinsic pseudospins from different Landau orbits which mix effectively give rise to multiple splitting of Landau levels. By incorporating Bloch wave function characteristics, we established an eigenvalue equation which yields fractal self-similar structure for the allowed energy band structure determined by the orbital pseudospin and magnetic field

signatures. In our calculations for the density of states, the physical origins of self-similarity are clearly established as being accessible experimentally. In particular, the emergence of Hofstadter's butterfly spectrum lies within a reasonable range of magnetic field that is currently available. Our numerical results clearly demonstrate magnetic field control of the energy density locations of the charge carriers and provide a basis for future experiments where regions of high absorption and conductivity may be observed at certain field strength. On the contrary, in the absence of magnetic field, the density-of-state lines are aligned next to each other.

ACKNOWLEDGMENT

[1] B. Hunt, J. D. Sanchez-Yamagishi, A. F. Young, M. Yankowitz, B. J. LeRoy, K. Watanabe, T. Taniguchi, P. Moon, M. Koshino, P. Jarillo-Herrero, and R. C. Ashoori, Science **340**, 1427 (2013).

[2] C. R. Dean, L. Wang, P. Maher, C. Forsythe, F. Ghahari, Y. Gao, J. Katoch, M. Ishigami, P. Moon, M. Koshino, T. Taniguchi, K. Watanabe, K. L. Shepard, J. Hone, and P. Kim, Nature (London) **497**, 598 (2013).

[3] L. A. Ponomarenko, R. V. Gorbachev, G. L. Yu, D. C. Elias, R. Jalil, A. A. Patel, A. Mishchenko, A. S. Mayorov, C. R. Woods, J. R. Wallbank, M. Mucha-Kruczynski, B. A. Piot, M. Potemski, I. V. Grigorieva, K. S. Novoselov, F. Guinea, V. I. Fal'ko, and A. K. Geim, Nature (London) **497**, 594 (2013).

[4] M. Ya. Azbel, Zh. Eksp. Teor. Fiz. **46**, 939 (1964) [Sov. Phys. JETP **19**, 634 (1964)].

[5] D. R. Hofstadter, Phys. Rev. B **14**, 2239 (1976).

[6] J. Jung, A. DaSilva, S. Adam, and A. H. MacDonald, arXiv:1403.0496.

[7] C. R. Woods, L. Britnell, A. Eckmann, R. S. Ma, J. C. Lu, H. M. Guo, X. Lin, G. L. Yu, Y. Cao, R. V. Gorbachev, A. V. Kretinin, J. Park, L. A. Ponomarenko, M. I. Katsnelson, Yu. N. Gornostyrev, K. Watanabe, T. Taniguchi, C. Casiraghi, H-J. Gao, A. K. Geim, and K. S. Novoselov, Nat. Phys. **10**, 451 (2014).

[8] Andrew L. C. Hayward, Andrew M. Martin, and Andrew D. Greentree, Phys. Rev. Lett. **108**, 223602 (2012).

[9] S. Janecek, M. Aichinger, and E. R. Hernández, Phys. Rev. B **87**, 235429 (2013).

[10] Pilkyung Moon and Mikito Koshino, Phys. Rev. B **85**, 195458 (2012).

[11] R. Bistritzer and A. H. MacDonald, Phys. Rev. B **84**, 035440 (2011).

[12] Z. F. Wang, Feng Liu, and M. Y. Chou, Nano Lett. **12**, 3833 (2012).

[13] M. Kindermann and E. J. Mele, Phys. Rev. B **84**, 161406(R) (2011).

[14] Godfrey Gumbs and Paula Fekete, Phys. Rev. B **56**, 3787 (1997).

[15] G. H. Wannier, Phys. Status Solidi B **100**, 163 (1980).

[16] A. Rauh, G. H. Wannier, and G. Obermair, Phys. Status Solidi B **63**, 215 (1974).

[17] A. Rauh, Phys. Status Solidi B **69**, K9 (1975).

[18] H. W. Neumann and A. Rauh, Phys. Status Solidi B **96**, 233 (1979).

[19] Y. Hasegawa, Y. Hatsugai, M. Kohmoto, and G. Montambaux, Phys. Rev. B **41**, 9174 (1990).

[20] Y. Hatsugai and M. Kohmoto, Phys. Rev. B **42**, 8282 (1990).

[21] D. Pfannkuche and R. R. Gerhardts, Phys. Rev. B **46**, 12606 (1992).

[22] D. Pfannkuche and R. R. Gerhardts, Surf. Sci. **263**, 324 (1992).

[23] D. J. Thouless, Phys. Rev. B **28**, 4272 (1983).

[24] F. Claro, Phys. Status Solidi B **104**, K31 (1981).

[25] H. J. Schellnhuber and G. M. Obermair, Phys. Rev. Lett. **45**, 276 (1980).

[26] G. Petschel and T. Geisel. Phys. Rev. Lett. **71**, 239 (1993).

[27] X. Wu and S. E. Ulloa, Phys. Rev. B **47**, 10028 (1993).

[28] H. Silbernauer, J. Phys.: Condens. Matter **4**, 7355 (1992).

[29] J. B. Sokoloff, Phys. Rep. **126**, 189 (1985).

[30] O. Kühn, V. Fessatidis, H. L. Cui, P. E. Selbmann, and N. J. M. Horing, Phys. Rev. B **47**, 13019(R) (1993).

[31] N. Nemec and G. Cuniberti, Phys. Rev. B **75**, 201404(R) (2007).

[32] S. Dröscher, P. Roulleau, F. Molitor, P. Studerus, C. Stampfer, K. Ensslin, and T. Ihn, Appl. Phys. Lett. **96**, 152104 (2010).

[33] P. D. Ye, D. Weiss, R. R. Gerhardts, M. Seeger, K. von Klitzing, K. Eberl, and H. Nickel, Phys. Rev. Lett. **74**, 3013 (1995).

[34] M. Zarenia, P. Vasilopoulos, and F. M. Peeters, Phys. Rev. B **85**, 245426 (2012).

[35] Godfrey Gumbs, Andrii Iurov, Danhong Huang, Paula Fekete, and Liubov Zhemchuzhna, AIP Conf. Proc. **1590**, 134 (2014).

[36] N. Nemec and G. Cuniberti, Phys. Rev. B **74**, 165411 (2006).

[37] L. Brey and H. A. Fertig, Phys. Rev. Lett. **103**, 046809 (2009).

[38] Li-Gang Wang and Shi-Yao Zhu, Phys. Rev. B **81**, 205444 (2010).

[39] L. Z. Tan, C.-H. Park, and S. G. Louie, Phys. Rev. B **81**, 195426 (2010).

[40] Danhong Huang, Godfrey Gumbs, and Norman J. M. Horing, Phys. Rev. B **49**, 11463 (1994).